Axial Dispersion During Pulsating Pipe Flow

HARRY M. TAYLOR and EDWARD F. LEONARD

Columbia University, New York, New York

A method is developed for the treatment of data obtained from flow systems whose performance is unsteady and periodic. Experimental results from a study of axial dispersion in pulsating turbulent flow in an open, round pipe are presented; they show that pulsations can greatly increase axial mixing.

In the last decade residence time methods have been extensively applied to the analysis of steady state systems, particularly to the flow performance of open and packed tubes. To the authors' knowledge the method has not, however, been deliberately applied to systems without steady state flow, probably because of both conceptual and experimental problems that such systems present. The investigation of flow systems whose performance is unsteady but periodic is of both practical and fundamental importance, and the flow behavior of such systems is not well understood. Since much industrial pumping is performed by reciprocating pumps, practical use can be made of information about unsteady, periodic flow in pipes to predict intermixing of separate streams carried in the same pipeline or for a variety of other calculations involving knowledge of axial dispersion.

In addition to the direct reasons for studying unsteady systems, there is an important but more subtle additional reason for such residence time studies; that is the concern that has been expressed about how to interpret residence time functions obtained from supposedly steady state systems when replicate measurements of these functions show considerable variations. Such differences often arise from a pseudo steady state behavior in which more or less random and, in some cases, large departures from true steady state occur during measurement. Large-scale turbulence and other manifestations of metastability may cause such irreproducibility. For many purposes averaging replicate results may lead to an incorrect interpretation of system performance. The study of systems subjected to deliberate flow disturbances may contribute to a better understanding of this problem as well as the more general problem of unsteady state systems.

To date treatment of the experimental information obtained on pulsating systems has been limited to empirical approaches, with very little theoretical treatment. Numerous authors have reported that pulsing enhances mass transfer in extraction columns (*1, 2, 3*) as well as natural convective heat and mass transfer (*4, 5*).

While no work has been done toward the theoretical treatment of dispersion in pulsating turbulent flow, Aris (*6*) has presented an elegant mathematical study of pulsating laminar flow dispersion. In this study he found that the effect of pulsing flow is unimportant unless the amplitude of the pressure gradient fluctuations is larger than the mean pressure gradient. This theoretical result for pulsating laminar flow is in sharp contrast to the experimental findings for pulsating turbulent flow reported below.

EXPERIMENTAL

In the present study cyclic flow variations were imposed on water flowing turbulently through an open, round pipe (0.250 in. I.D.). The system is shown in Figure 1. Dye (Azo Scarlet Y) and water were mixed so as to produce a stream of constant flow rate but sinusoidally varying dye concentration. This stream was passed through a small pump and then through a length of flexible tubing (see inset, Figure 1) that could be alternately collapsed and expanded by application of air pressure to a rigid containing chamber. Dye concentrations were monitored optically at two stations, spaced 18.8. ft. apart in the pipe, by photomultiplier tubes (CBS type 7817). The monitoring stations were constructed of clear acrylic plastic that had been bored and polished to the same inner diameter as the pipe. The pipe was extended 15 in. beyond the inlet and outlet monitoring stations to reduce end effects. Flow variations were measured by a turbine flowmeter (Pottermeter) located 15 in. beyond the outlet monitoring station.

An on-line analog computer transformed light intensity signals into voltages proportional to concentration. Sample traces of the inlet and outlet sinusoids obtained for steady flow are shown in Figure 2. Flow signals were also processed by the computer to obtain the integral of the varying part of the flow, as required in the analysis described below (*7*).

DATA PROCESSING

To illustrate the method for treating pulsing flow data, consider a one-dimensional system of doubly infinite extent in whch fluid is flowing at a velocity $U(t)$ and on which a concentration function

$$C(t) = A_i \sin \omega t \qquad (1)$$

is imposed at the point $x = 0$. For steady flow [that is, for $U(t)$ constant] the concentration at some point $x = S$, $(S > 0)$ is then given by

$$C(t) = A(S) \sin (\omega t + \Phi) \qquad (2)$$

which is still a pure sinusoid having a phase lag Φ with respect to the inlet sinusoid. If, however, the flow is pul-

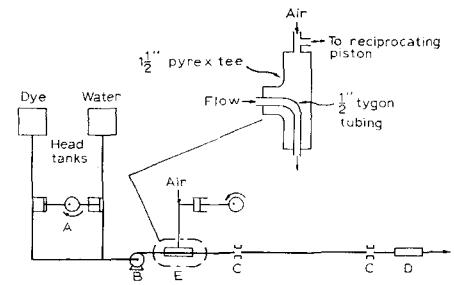

Fig. 1. Flow system schematic showing details of pulsing station.

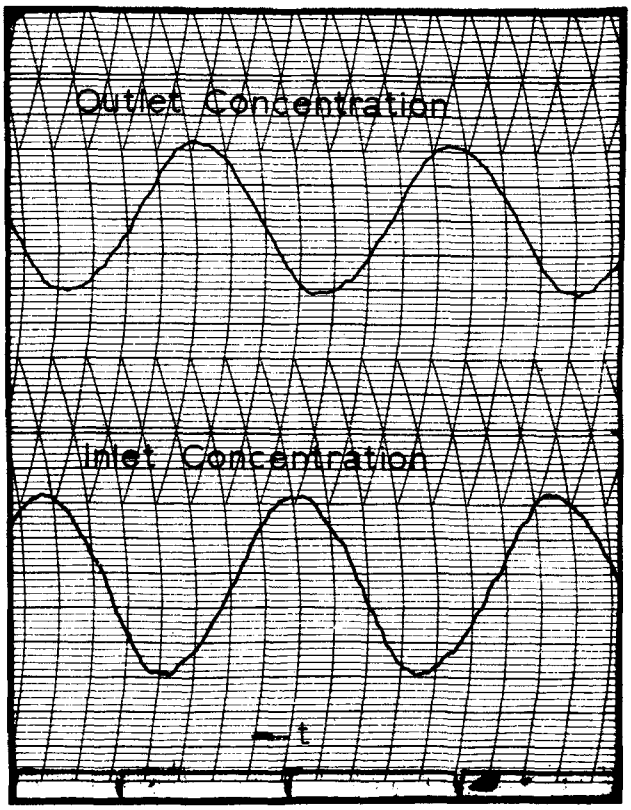

Fig. 2. Tracing obtained from steady flow system.

sating, the concentration-time function observed at any point will be distorted by the variations in the fluid velocity. The following development shows how it has been possible to account for these distortions while still recognizing the effect of the flow variations on axial mixing.

For a periodic velocity function of the form (see Figure 3*a* as an example)

$$U(t) = U_o + \tilde{U}(t) \tag{3}$$

a tracer particle will travel by convection in time t a distance $S(t)$

$$S(t) = \int_0^t U(t')\, dt' \tag{4}$$

A sample of the function $S(t)$ is plotted in Figure 3*b*.

Cross plotting the two curves shown in Figures 3*a* and 3*b* gives the velocity as a function of distance traveled, illustrated by Figure 4*a*. The age of a particle at any point S is then given by

$$T_s = \int_0^s \frac{dS'}{U(S')} \tag{5}$$

However, as

$$\int_0^t U_o\, dt >> \int_0^t \tilde{U}(t)dt \tag{6}$$

S' becomes approximately linear in t and Equation (5) may be approximated as

$$T_s \cong \overline{T}_s = \int_0^s \frac{dS'}{U_o} = \frac{S}{U_o} \tag{7}$$

The quantity $\overline{T}_s$ is a constant for any given S and implies that the response amplitude $A(S)$ will be constant for any S. Use of $\overline{T}_s$ for T_s in the analysis of dispersion during pulsating flow amounts to assuming that no mixing occurs during a period of time equal to the difference between the time of arrival at the observation point due to the mean flow and that time actually observed for pulsing flow. This time difference is given by

$$\tilde{T}_s(t) = \frac{1}{U_o}\int_0^t \tilde{U}(t)dt \tag{8}$$

where t is actual time at any instant. Figure 4*b* shows the relative behavior of T_s and $\overline{T}_s$.

Since the maximum value of Equation (8) occurs at the half period of $\tilde{U}(t)$, it is obvious that for any given amplitude of $\tilde{U}(t)$ the maximum value of $\tilde{T}_s(t)$ decreases as the flow rate and pulsation frequency are increased. When mixing over $\tilde{T}_s$ is negligible compared with that which has taken place over $\overline{T}_s$, distortion of the concentration-distance waveform is minor.

Then one needs only to allow for the fact that the fluid is going to reach some fixed observation point sooner or later than the mean residence time by an amount equal to the instantaneous value of $\tilde{T}_s(t)$, and that the concentration-time function measured at a fixed point will not be sinusoidal in t but rather will be given by

$$C(t) = A(S)\sin\{\omega(t + \tilde{T}_s(t)) + \Phi\} \tag{9}$$

For the simple case of a constant velocity, this equation reduces to Equation (2). Thus, we define a new time scale

$$\tau = t + \tilde{T}_s(t) \tag{10}$$

Plotting experimental values of $C(S,t)$ as $C(S,\tau)$ should then transform the response to a sinusoidal form. This approach and assumption of negligible mixing over the time $\tilde{T}_s$ are vindicated if the resulting waveform approximates well a sinusoid of the forcing frequency.

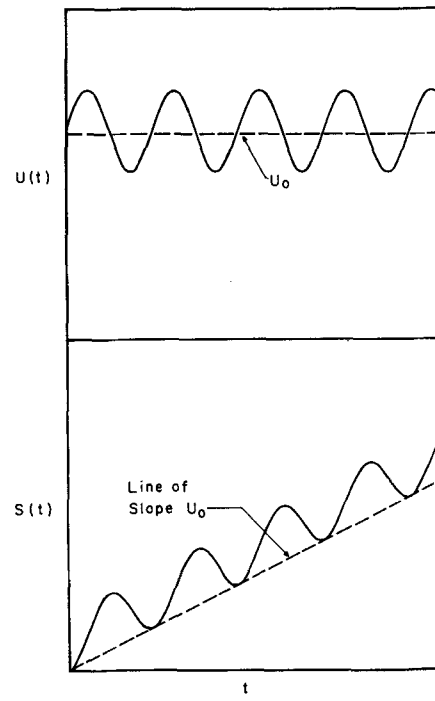

Fig. 3*a* (top). A typical cyclic velocity variation showing $U(t) = U_o + |\tilde{U}(t)|\sin\Omega t$. Fig. 3*b* (bottom). $S(t)$ for a tracer particle flowing at the velocity $U(t)$.

The experimental data were obtained as strip-chart recordings of the inlet and outlet concentration-time functions, the velocity variations, and the integrated velocity variations. These data were then manually digitized for processing on an IBM 7090 computer. For every concentration forcing-frequency 150 points were read for each of the inlet and outlet concentration functions and for the integrated velocity function. These readings encompassed from four to six cycles of the concentration variations and from two to twelve cycles of the velocity integral function, depending on the chart drive speed.

Once the data were digitized the computer was programmed to fit Fourier time series to each of the three functions simultaneously and to transform the concentration-time functions according to the scheme outlined above. Finally, the machine was instructed to fit another Fourier series to the transformed data, from which the desired concentration functions were extracted. The program was tested with "perfect" sample data and found to be accurate within 0.2%. Twelve harmonics were fitted to the concentration functions and six to the velocity integral function. Both the steady and unsteady flow runs reported below were processed identically to allow proper comparisons. Process noise, as revealed by the Fourier harmonics, was such as to allow analysis of the steady flow data for concentration frequencies up to 120 cycles/min. The unsteady flow noise level, however, became sufficiently high above 60 cycles/min. to prevent analysis beyond this point.

RESULTS

Because facilities for the facile reduction of experimental data were not available, only one pair of experimental runs was made, one with and one without flow pulsation, under otherwise identical conditions. The primary problem in the data reduction stemmed from digitizing the data manually. It is the authors' feeling that with automatic analog-to-digital conversion capabilities the data reduction could be accomplished relatively easily.

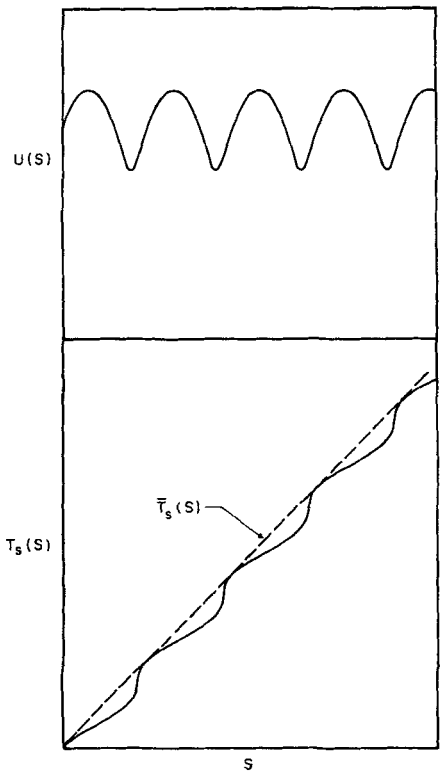

Fig. 4a (top). Tracer particle velocity as a function of S. Fig. 4b (bottom). Tracer particle "age" as a function of S.

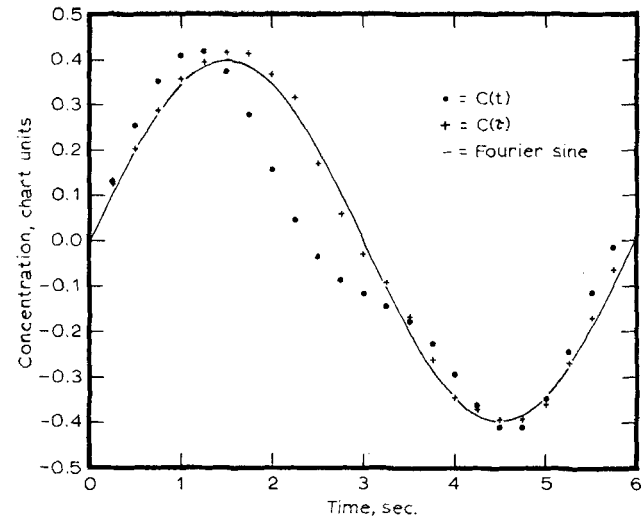

Fig. 5. Comparison of unprocessed data C(t) and transformed data C(τ), showing the fundamental sine wave yielded by Fourier analysis of C(τ).

The effectiveness of the transformation technique outlined above is illustrated in Figure 5. While the transformed data points do not constitute a perfect sine wave, it is obvious that they are a far better approximation to one than are the unprocessed data. Also they conform rather closely to the fundamental sine wave found by the final Fourier analysis.

Figure 6 shows a typical set of tracings obtained from the unsteady flow system, illustrating the pulsing distortions to the inlet and outlet concentration-time waveforms. The drift shown in the tracing for the velocity integral function is due to a very small, slow variation in the mean flow velocity. The frequency response curves obtained from the analysis of such tracings for both pulsing and steady flow are shown in Figure 7. For both cases the Reynolds number based on mean flow velocity was 15,500. The peak-to-peak velocity variations for the pulsing curve corresponded to 14.6% of the mean flow velocity (U_o = 8.96 ft./sec.). The pulsing frequency was 0.4 cycles/sec.

It is obvious from these results that axial dispersion was greatly enhanced by the pulsations. Analysis of the data indicated that the physical situation with and without pulsing was adequately described by the model for piston flow with axial diffusion, given by

$$\frac{\partial^2 C}{\partial x^2} - \frac{U_o}{D}\frac{\partial C}{\partial z} - \frac{1}{D}\frac{\partial C}{\partial t} = 0 \qquad (11)$$

Earlier studies using this model (8) have shown that for a sinusoidal input in concentration the amplitude ratio, $\alpha(\omega)$, and phase lag, $\Phi(\omega)$, of the concentration-time waveform for a test length S can be approximated by

$$\alpha(\omega) = \exp\left[\frac{\omega^2 DS}{U_o^3} + \frac{5\omega^4 D^2 S}{U_o^7} + \ldots\right] \qquad (12)$$

$$\Phi(\omega) = \left[-\frac{\omega S}{U_o} + \frac{2\omega^3 D^2 S}{U_o^5} + \ldots\right] \qquad (13)$$

Using only the first term in each of these expansions, the amplitude ratio and phase lag functions were found to be

$$\alpha(\omega)_{\text{pulsing}} = \exp\left[-0.0354\omega^2\right]$$
$$\Phi(\omega)_{\text{pulsing}} = -2.25\omega$$
$$\alpha(\omega)_{\text{steady}} = \exp\left[-0.00322\omega^2\right]$$
$$\Phi(\omega)_{\text{steady}} = -2.09\omega$$

where ω is the concentration forcing frequency in radians/sec. The effective axial diffusion coefficients were found to be 1.36 sq. ft./sec. for unsteady flow and 0.123 sq. ft./sec. for steady flow. While no previous coefficients have been reported for pulsing flow, the steady flow coefficient compares favorably with values reported by Tichacek et al. (9).

Not only the steady but also the pulsing flow frequency spectra were found to fit well the truncated forms of (12) and (13), indicating that the marked augmentation of dispersion could still be described by an axial dispersion coefficient, and suggesting that the mechanism of dispersion coefficient may not be radically different. Analysis of the theory for axial dispersion in steady turbulent flow (9, 10) suggests three possible reasons for the greatly enhanced dispersion observed in this work. Either (1) in pulsing flow the axial eddy diffusivity is very much larger, or (2) the radial diffusivity is very much smaller, or (3) the time-average curvature of the velocity profile is greater than in steady flow. The measurements necessary to select from these alternatives have not, to the authors' knowledge, been made. However, it is difficult to see how direct axial dispersion can have an effect that is negligible in steady flow and yet dominant in pulsing flow. It is also hard to see how pulsing flow can decrease the radial diffusivity. While this work certainly falls short of demonstrating the fact, increased average curvature of the velocity distribution seems to be the most plausible explanation.

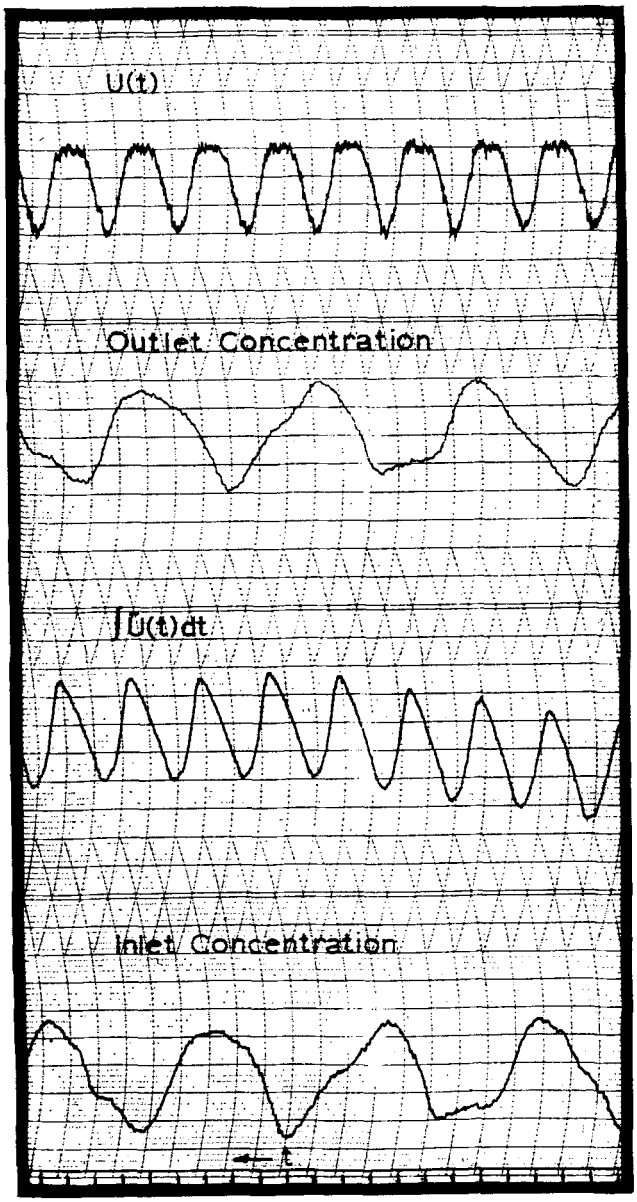

Fig. 6. Actual recorder tracing showing the distortions of the inlet and outlet concentration sine waves due to the pulsing.

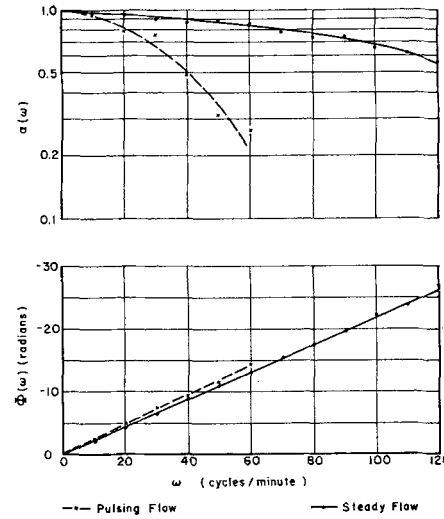

Fig. 7. Frequency response diagrams for the steady and pulsing flow cases investigated.

NOTATION

A_i = input concentration amplitude, dimensionless
$A(s)$ = concentration amplitude at S, dimensionless
$C(t)$ = tracer concentrations, dimensionless
D = effective axial diffusion coefficient, sq. ft./sec.
$S(t)$ = position coordinate, ft.
t = time, sec.
$T_s(t)$ = actual age of tracer at S, sec.
$\overline{T}_s$ = "average" age of tracer at S, sec.
$\tilde{T}_s(t)$ = variable part of $T_s(t)$, sec.
$U(t)$ = instantaneous flow velocity, ft./sec.
U_o = average flow velocity, ft./sec.
$\tilde{U}(t)$ = variable part of $U(t)$, ft./sec.
x = length coordinate, ft.

Greek Letters

$\alpha(\omega)$ = ratio of outlet to inlet concentration amplitudes, dimensionless
$\Phi(\omega)$ = phase lag, radians
τ = time, scale, corrected for pulsations, sec.
ω = concentration forcing frequency, radians/sec.

LITERATURE CITED

1. Li, W., and W. Newton, *A.I.Ch.E. J.*, **3**, 56 (1957).
2. Mar, B. W., and A. L. Babb, *Ind. Eng. Chem.*, **51**, 1011 (1959).
3. Moon, J., A. Hennico, and T. Vermeulen, *Rept. UCRL-10928*, Lawrence Radiation Laboratory (1963).
4. Lemlich, R., *Ind. Eng. Chem.*, **47**, 1175 (1955).
5. ———, and M. Levy, *A.I.Ch.E. J.*, **7**, 240 (1961).
6. Aris, R., *Proc. Roy. Soc.*, **A259**, 370 (1960).
7. Taylor, H. M., M.S. thesis, Columbia Univ., New York (1963).
8. McHenry, K., and R. Wilhelm, *A.I.Ch.E. J.*, **3**, 83 (1957).
9. Tichacek, L., C. Barkelew, and R. Baron, *ibid.*, 439.
10. Taylor, G. I., *Proc. Roy. Soc.*, **A223**, 446 (1954).

Manuscript received September 22, 1964; revision received January 21, 1965; paper accepted March 10, 1965.